Available online at www.sciencedirect.com

ScienceDirect

Acta Materialia 75 (2014) 113–121

Acta MATERIALIA

www.elsevier.com/locate/actamat

Determining characteristic principal clusters in the "cluster-plus-glue-atom" model

Jinglian Du [a], Bin Wen [a,*], Roderick Melnik [b], Yoshiyuki Kawazoe [c,d]

[a] State Key Laboratory of Metastable Materials Science and Technology, Yanshan University, Qinhuangdao 066004, China
[b] M^2NeT Lab, Wilfrid Laurier University, Waterloo, 75 University Ave West, Ontario N2L 3C5, Canada
[c] New Industry Creation Hatchery Center, Tohoku University, 6-6-4 Aramaki-aza-Aoba, Aoba-ku, Sendai 980-8579, Japan
[d] Institute of Thermophysics, Siberian Branch of the Russian Academy of Sciences, 1 Lavyrentyev Avenue, Novosibirsk 630090, Russia

Received 5 March 2014; received in revised form 21 April 2014; accepted 21 April 2014
Available online 2 June 2014

Abstract

The "cluster-plus-glue-atom" model can easily describe the structure of complex metallic alloy phases. However, the biggest obstacle limiting the application of this model is that it is difficult to determine the characteristic principal cluster. In the case when interatomic force constants (IFCs) inside the cluster lead to stronger interaction than the interaction between the clusters, a new rule for determining the characteristic principal cluster in the "cluster-plus-glue-atom" model has been proposed on the basis of IFCs. To verify this new rule, the alloy phases in Cu–Zr and Al–Ni–Zr systems have been tested, and our results indicate that the present new rule for determining characteristic principal clusters is effective and reliable.

Keywords: "Cluster-plus-glue-atom" model; Interatomic force constants; Principal cluster

1. Introduction

Cluster-based models [1–6] have been proposed to describe the structure of quasi-crystalline and amorphous alloys, since for a long time the coordinate polyhedral clusters were advocated as the basic primary units to reflect the structure characteristics of materials [7–11]. As for the complex metallic alloy phases, the structures of which are difficult to determine, the cluster information and local atomic structure characteristics can be obtained approximately from the related crystalline phases [12–14]. Meanwhile, clusters act as the basic building unit of materials and their hard-sphere packing has been addressed by a series of experiments and simulations [15–17], with a view to determining the structural models and understanding the structural information of complex alloy phases. Recently, Dong et al. [18–20] and Han et al. [21] have proposed a "cluster-plus-glue-atom" model to describe the structure of complex metallic alloy phases. Compared with the traditional classical crystallography [22–25], the "cluster-plus-glue-atom" model can simultaneously describe both the structural and componential information of the researched materials. It also has a wide range of applications. One of the most important applications is that it provides a feasible approach for the compositional design of complex metallic alloy phases in a quantitative manner, since both the structural and componential information can be conveniently obtained from the model configuration [6]. Meanwhile, this application has been verified systematically on the basis of theoretical and experimental analyses [26–35]. Concisely, the "cluster-plus-glue-atom" model can be expressed as a uniform cluster formula, [cluster](glue atoms)$_x$, where cluster refers to the basic near-neighbor

* Corresponding author. Tel.: +86 335 8568761.
E-mail address: wenbin@ysu.edu.cn (B. Wen).

http://dx.doi.org/10.1016/j.actamat.2014.04.052
1359-6454/

coordinate polyhedron derived from the corresponding crystalline phases, glue atoms are regarded as the interstitial filling between clusters and x is the number of glue atoms matching one cluster [1,19,20]. As a consequence, the structures of materials can be divided into the cluster part and the glue atoms part. Subsequently, all the atoms in a given structure can be classified into three categories, i.e. the glue atoms, the central atom and the shell atoms of clusters, as shown in Supplementary Fig. S1.

According to this cluster-based model, designing complex metallic alloy phases with optimal composition is considered to be feasible under the assumption that the configurations of the stable characteristic principal clusters in the complex metallic alloys and their crystalline derivatives remain similar to each other [36–49]. Hence, it is no wonder that the structural analysis of crystalline phases becomes the foundation of this cluster-based model, and determination of the characteristic principal clusters together with the linkage rules become the start-points to apply the model. Accordingly, the first step is to obtain the basic primitive clusters from the related crystalline phase, while the second step is to determine the characteristic principal cluster reflecting the structural feature of the phase [50–52]. Since a dense-packed cluster with its own coordination number (CN) can be defined around any non-equivalent atomic position in the unit cell of a phase, the most representative principal cluster needs to be selected and be used to further describe the relevant metallic complex alloy phases.

Over the years, much effort has been made to develop of the characteristic principal cluster's selection criteria [53–55]. However, these are not as distinctive as anticipated. Therefore, the rules for establishing the appropriate characteristic principal cluster still need further investigation. Since the interaction between atoms inside the cluster is stronger than that between clusters corresponding to the glue atoms [2,20,28,30,56], the interatomic force constants (IFCs), which can be used to reflect the interaction between atoms, is proposed as a way to describe the "cluster-plus-glue-atom" model. In this study, IFCs have been obtained by performing first-principles calculations within the framework of density functional perturbation theory, with particular emphasis on the determination of appropriate characteristic principal clusters for the "cluster-plus-glue-atom" model, combined with the existing criteria [53–55]. The alloy phases in Cu–Zr and Al–Ni–Zr [52,53,57–59] systems have been checked for this application. The results indicate that, through calculation and analysis of IFCs, the central atom as well as the shell atoms of the cluster and the glue atoms can be distinguished; a suitable characteristic principal cluster can thus be effectively established by combining the existing rules.

The remainder of the paper is organized as follows. In Section 2, we briefly review previous selection rules for the characteristic principal cluster. In Section 3, the proposal of a new rule for establishing characteristic principal clusters in the "cluster-plus-glue-atom" model is deciphered. In Section 4, the alloy phases in Cu–Zr and Al–Ni–Zr systems are checked to verify this new rule. Finally, the conclusion and outlook are given in Section 5.

2. Review of previous selecting rules for the characteristic principal cluster

2.1. Close-packing principle

The structural characteristics of materials can be reflected well by the most close-packed cluster, given that the close-packing of atoms is a fundamental requirement for structural stability [52,55,60,61]. Accordingly, in the "cluster-plus-glue-atom" model, clusters should be the most close-packed part, thus the cluster characteristic can be reflected well [55]. Therewith, the cluster packing fraction and packing efficiency have been proposed as two measurable criteria to reflect the close-packing properties of materials [62]. Generally, the atomic packing properties can be reflected well by these two criteria. However, the packing fractions are not sensitive to cluster type or atom type, so it is not a suitable parameter for cluster close-packing reflects. Besides, the packing efficiency of atoms can be considered as an effective criterion describing the packing properties of real clusters [55]. Also, Miracle and colleagues obtained the critical radius ratios R^* to evaluate the packing efficiency of an ideal cluster shelled by one type of atoms, assuming perfect spherical contact between atoms [2,4,5]. Nevertheless, in some cases where different shells are possible, the distinctions reflected by the packing efficiency criterion to elucidate the confusion in cluster selection are not significant, and this criterion still holds true as a simple approximation. Therefore, other close-packing criteria still need to be developed to determine the characteristic principal clusters.

Research has indicated that radial atomic density can be considered as a feasible criterion to assess the close-packing property of atoms [54]. Hence, the near-neighbor coordination polyhedron composed of atoms is selected before the shells with the maximum radial atomic density as the first close-packing cluster; this implies that the cluster is the local atomic structure with the highest structural density [55]. Furthermore, the structural integrity, referring to the concept that a close-packing cluster is normally enclosed with surface triangular facets, should also be taken into consideration. The radial atomic density is defined to be the number of atoms per unit volume and reflected by $\rho_a = N/V_{cluster}$, where N is the number of atoms enclosed by a sphere with volume $V_{cluster}$. Therewith, the cut-off cluster shell should locate near the maximum ρ_a [54]. Taking the $CuZr_2$ alloy phase as an example, there are one Cu and one Zr non-equivalent atomic site in the $CuZr_2$ unit cell. Hence, the basic primitive clusters centered by the Cu atom and Zr atom can be defined. Correspondingly, the radial atomic density distributions of clusters centered by the Cu atom and Zr atom are plotted in Fig. 1a and b, respectively. The cut-off cluster shell centered by Cu is

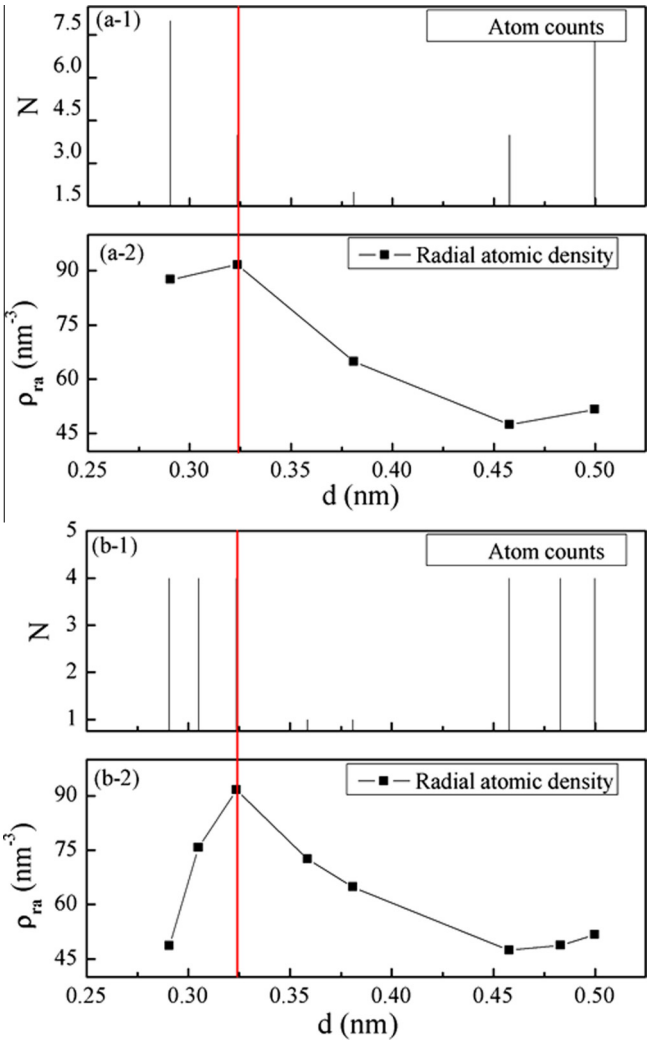

Fig. 1. The distribution of radial atomic distances and radial atomic densities for the (a) Cu and (b) Zr sites in the $CuZr_2$ alloy phase. The red solid vertical line points the cutoff cluster shells.

located near the maximum ρ_a so that CN12 Cu_5Zr_8 is the appropriate cluster. Similarly, the CN12 Zr_9Cu_4 is regarded as the suitable cluster for a Zr-centered near-neighbor coordinate polyhedron. The typical structures for a $CuZr_2$ unit cell, and Cu-centered as well as Zr-centered near-neighbor coordinate polyhedral clusters, are shown in Supplementary Fig. S2. In this study, the first element in the cluster is the central atom of the cluster.

In addition, given that the near-neighbor shell of clusters is usually spread over a few layers, the distribution of the first shell reflected by $k = (r_{max} - r_{min})/r_{max}$ is considered to be another criterion to evaluate the degree of structural perfection of the clusters, with r_{max} and r_{min} denoting the maximum and minimum radial distances of the first shells, respectively [32]. Evidently, a relatively narrow distribution of the cluster shell atoms often implies a better enclosed and hence a more close-packed cluster. Thus, a smaller rather than a larger k is preferred and all atoms within the cutoff radius are considered as the first near-neighbor shell of the central atom.

2.2. Enthalpies of mixing and atomic size differences

The strong interaction between atoms is necessary for different elements forming a near-neighbor coordinate polyhedral cluster [33]. Therewith, the enthalpy of mixing ($\triangle H$) can be used to reflect the interactions between elements, and a negative value indicates an attractive interaction, while a positive value implies a repulsive interaction between elements [63–67]. Accordingly, the elements with negative enthalpy of mixing tend to form the short-range order atomic clusters. In the "cluster-plus-glue-atom" model, the cluster is the strongly interacted part centered by the element having negative enthalpy of mixing with the shell atoms, whereas the glue atoms are relative weakly interacting with the cluster shell atoms, and are preferentially composed of elements having positive enthalpy of mixing with the central atom of the cluster. Therefore, in alloy phases consisting of negative enthalpies of mixing and obvious atomic size differences, dissimilar atoms tend to form the first near-neighbor coordination polyhedral clusters, and these clusters constitute the local atomic features of the formed phases [15,20,30,35,52]. The cluster's definition can also be understood in terms of the atomic size differences. Nevertheless, the consideration of atomic radius is usually empirical given that the real atomic radius may change due to the strong chemical interactions between atoms. Thus, factors other than enthalpies of mixing and atomic size differences should be incorporated in the process of establishing the characteristic principal cluster. In doing this, researchers may reveal interesting properties common to the "cluster-plus-glue-atom" model.

As mentioned above, the appropriate characteristic principal cluster can be distinguished from various basic primitive clusters on the basis of atomic close-packing, enthalpy of mixing and atomic size differences. However, the distinctions of principal cluster based on these criteria are not as obvious as expected, especially for the complex crystalline alloy phases. Therefore, certain rules for determining the characteristic principal clusters still need further investigations. In the following part, we will introduce a new method to establish the appropriate characteristic principal cluster for the "cluster-plus-glue-atom" model from the viewpoint of the interaction between atoms reflected by the parameter IFCs.

3. A new rule to determine the characteristic principal clusters in the cluster-plus-glue-atom model

Researchers have found that in the "cluster-plus-glue-atom" model, the interaction between atoms inside the cluster is stronger than that between clusters corresponding to the glue atoms [2,20,28,30,56]. To better understand this fact, we have investigated the variation trend of near-neighbor interatomic spacing as a function of hydrostatic pressure for the Al_2NiZr_6 alloy phase. In terms of Al_2NiZr_6, the characteristic principal cluster is regarded as Ni-centered CN11 Ni_3Zr_9 and the glue atom is Al. The near-neighbor

interatomic spacing, as a function of the pressure between atoms inside the cluster Ni–Zr and that between the clusters Zr–Al, is depicted in Supplementary Fig. S3. As is shown, the near-neighbor interatomic spacing decreases as the hydrostatic pressure increases. Furthermore, the corresponding variation trend for atoms inside the cluster Ni–Zr is slower than that between the clusters corresponding to Zr–Al. This result indicated that the interaction between atoms inside the cluster is stronger indeed than that between the clusters corresponding to the glue atoms. Accordingly, the parameter IFCs, which can be used to reflect the interactions between atoms, is proposed to describe the "cluster-plus-glue-atom" model in this study.

IFCs are the coefficients describing the force created on one atom by the displacement of another atom from its equilibrium position in a linear order; i.e. when one atom is displaced from its equilibrium position, it exerts a force on other atoms and, through induction, a restoring force acts upon the atom itself. The scale factor of the displacement and the force between atoms are viewed as the IFCs [68]. As for the nature of this parameter, IFCs are defined as the second order derivatives of the ground-state energy for the researched system with respect to atomic displacement [69]. For example, with regard to a system containing two atoms, which are labeled as ① and ②, when displacement $\delta\overrightarrow{r_2} = (\delta x_2, \delta y_2, \delta z_2)$ is caused by atom ②, the corresponding force $\delta\overrightarrow{F}_1 = (\delta F_{x_1}, \delta F_{y_1}, \delta F_{z_1})$ exerted on atom ① can be described by:

$$\delta\overrightarrow{F_1} = [k_{12}]\delta\overrightarrow{r_2} \tag{1}$$

Specifically, it can be written as:

$$\delta F_1 = \begin{bmatrix} \delta F_{x_1} \\ \delta F_{y_1} \\ \delta F_{z_1} \end{bmatrix} = - \begin{bmatrix} \frac{\partial^2 E}{\partial x_1 \partial x_2} & \frac{\partial^2 E}{\partial x_1 \partial y_2} & \frac{\partial^2 E}{\partial x_1 \partial z_2} \\ \frac{\partial^2 E}{\partial y_1 \partial x_2} & \frac{\partial^2 E}{\partial y_1 \partial y_2} & \frac{\partial^2 E}{\partial y_1 \partial z_2} \\ \frac{\partial^2 E}{\partial z_1 \partial x_2} & \frac{\partial^2 E}{\partial z_1 \partial y_2} & \frac{\partial^2 E}{\partial z_1 \partial z_2} \end{bmatrix} \times \begin{bmatrix} \delta x_2 \\ \delta y_2 \\ \delta z_2 \end{bmatrix} \tag{2}$$

Accordingly, the IFCs can be deduced and presented as:

$$[k_{12}] = \frac{\delta\overrightarrow{F_1}}{\delta\overrightarrow{r_2}} \tag{3}$$

Similarly, as for a system containing N atoms, the force $\delta\overrightarrow{F}$ induced by the displacement $\delta\overrightarrow{r}$ can be expressed as:

$$\delta\overrightarrow{F} = [k]\delta\overrightarrow{r} \tag{4}$$

where the $3N \times 3N$ dimensional matrix $[k]$ is defined as the IFCs matrix and given as:

$$[k] = \begin{bmatrix} \frac{\partial^2 E}{\partial x_1^2} & \frac{\partial^2 E}{\partial x_1 \partial x_2} & \frac{\partial^2 E}{\partial x_1 \partial x_3} & \cdots & \frac{\partial^2 E}{\partial x_1 \partial x_{3N}} \\ \frac{\partial^2 E}{\partial x_2 \partial x_1} & \frac{\partial^2 E}{\partial x_2^2} & \frac{\partial^2 E}{\partial x_2 \partial x_3} & \cdots & \frac{\partial^2 E}{\partial x_2 \partial x_{3N}} \\ \frac{\partial^2 E}{\partial x_3 \partial x_1} & \frac{\partial^2 E}{\partial x_3 \partial x_2} & \frac{\partial^2 E}{\partial x_3^2} & \cdots & \frac{\partial^2 E}{\partial x_3 \partial x_{3N}} \\ \vdots & \vdots & \vdots & \ddots & \vdots \\ \frac{\partial^2 E}{\partial x_{3N} \partial x_1} & \frac{\partial^2 E}{\partial x_{3N} \partial x_2} & \frac{\partial^2 E}{\partial x_{3N} \partial x_3} & \cdots & \frac{\partial^2 E}{\partial x_{3N}^2} \end{bmatrix} \tag{5}$$

The linear response methods based on density functional theory are thought to be a powerful tool for seeking the lattice dynamic of materials and for exploring the nature of force constants that cannot be obtained experimentally [70]. In addition, IFCs have an exponential relation with interatomic spacing [71], and in the real space, only the "on-site" IFCs are affected [72]. Research has indicated that the decay of IFCs will be inversely proportional to the cube of interatomic spacing [73]. Accordingly, we make a simplification, considering the interactions induced by the atom itself and the corresponding IFCs as the main block, while the interactions induced by other atoms and the related IFCs are the minor concern in our study. Consequently, the IFCs can be expressed as follows:

$$IFCs = \sqrt{\left(\frac{\partial^2 E}{\partial x_i^2}\right)^2 + \left(\frac{\partial^2 E}{\partial y_i^2}\right)^2 + \left(\frac{\partial^2 E}{\partial z_i^2}\right)^2} \tag{6}$$

In Eq. (6), $\frac{\partial^2 E}{\partial x_i^2}$, $\frac{\partial^2 E}{\partial y_i^2}$ and $\frac{\partial^2 E}{\partial z_i^2}$ are the corresponding $\vec{x}$, $\vec{y}$ and $\vec{z}$ directional IFCs for the i atom of the researched system, respectively.

Accordingly, the characteristic principal clusters are selected based on the different interactions between atoms reflected by IFCs. And for a given alloy phase, it is noticed that atoms whose IFCs are the largest serve as the central atoms of the cluster, those atoms whose IFCs are the smallest act as the glue atoms of the model, while those atoms whose IFCs are located between the maximum and minimum values serve either as the shell atoms of the cluster or as the glue atoms of the model.

4. Verification of the new rule

To verify the effectiveness of the new rule, the characteristic principal clusters for alloy phases in Cu–Zr and Al–Ni–Zr systems have been studied by using this new rule. In this work, the geometry optimization and IFCs' calculation have been performed by the first-principles investigations, as implemented in the Vienne Ab initio Simulation Package (VASP) [74], and concrete computational details are provided in the Supplementary materials.

Here, we take the Cu_8Zr_3 phase as an example to explain its characteristic principal cluster's determination method. According to the crystallographic information of Cu_8Zr_3 phase, there are eight kinds of atomic positions in its unit cell, labeled as Cu^1, Cu^2, Zr^3, Cu^4, Cu^5, Cu^6, Cu^7 and Zr^8, respectively [75]. Thus, eight types of basic primitive clusters can be defined correspondingly on the basis of the cluster's selecting rules mentioned in Section 2. They are the Cu^1-centered CN12 Cu_8Zr_5 cluster, the Cu^2-centered CN13 $Cu_{10}Zr_4$ cluster, the Zr^3-centered CN14 Zr_3Cu_{12} cluster, the Cu^4-centered CN12 Cu_8Zr_5 cluster, the Cu^5-centered CN13 $Cu_{11}Zr_3$ cluster, the Cu^6-centered CN12 Cu_8Zr_5 cluster, the Cu^7-centered CN11 Cu_6Zr_6 cluster and the Zr^8-centered CN17 Zr_5Cu_{13} cluster, respectively. To select the characteristic principal cluster from these eight basic primitive clusters, the IFCs

Table 1
Cluster information, including IFCs, primitive cluster, cluster CN, radial atomic density (ρ_a), relative atomic density compared with the unit cell (ρ_{ra}), ratio of the central atom and shell atom's radii (R_0/R_1), cutoff radius of the cluster shell (k) and cluster formula for the crystalline phases in Cu–Zr alloy system.

Phase	Center atom	IFCs (eV Å^{-2})	Primitive cluster	R_0–R_1–R_2–R_3	CN	ρ_a (nm^{-3})	ρ_{ra}	R_0/R_1	k	Effective cluster	Cluster formula
Cu_2Zr	Cu^1	8.38	$Cu_{10}Zr_5$	$Cu^1Cu^1_3Cu^2_6Zr^3_3Zr^4_2$	14	98.483	1.545	0.918	0.204	Cu_2Zr_1	$[Cu_{10}Zr_5]$
	Cu^2	8.38	$Cu_{10}Zr_5$	$Cu^2Cu^2_3Cu^1_6Zr^4_3Zr^3_2$	14	98.483	1.544	0.918	0.204	Cu_2Zr_1	$[Cu_{10}Zr_5]$
	Zr^3	16.21	Zr_5Cu_{10}	$Zr^3Cu^1_6Cu^2_4Zr^4_4$	14	98.528	1.545	1.167	0.155	Zr_2Cu_4	$[Zr_5Cu_{10}]$
	Zr^4	16.21	Zr_5Cu_{10}	$Zr^4Cu^2_6Cu^1_4Zr^3_4$	14	98.528	1.545	1.167	0.155	Zr_2Cu_4	$[Zr_5Cu_{10}]$
CuZr	Cu^1	3.76	Cu_7Zr_8	$Cu^1Zr^1_8Cu^1_6$	14	101.522	1.791	0.875	0.134	Cu_1Zr_1	$[Cu_7Zr_8](Cu)$
	Zr^1	12.59	Zr_7Cu_8	$Zr^1Cu^1_8Zr^1_6$	14	101.522	1.791	1.129	0.134	Zr_1Cu_1	$[Zr_7Cu_8](Zr)$
Cu_5Zr	Cu^1	4.64	$Cu_{17}Zr_4$	$Cu^1Cu^2_{12}Zr^1_4$	16	151.204	2.084	0.941	0.043	Cu_5Zr_1	$[Cu_{17}Zr_4](Cu_3)$
	Cu^2	13.72	$Cu_{10}Zr_3$	$Cu^2Cu^2_6Cu^1_3Zr^1_3$	12	131.749	1.816	0.941	0.147	$Cu_{5/4}Zr_{1/4}$	$[Cu_{10}Zr_3](Cu_5)$
	Zr^1	10.95	$ZrCu_{16}$	$Zr^1Cu^2_{12}Cu^1_4$	16	151.204	2.084	1.25	0.043	Zr_1Cu_5	$[ZrCu_{16}](Zr_{11/5})$
Cu_8Zr_3	Cu^1	10.75	Cu_8Zr_5	$Cu^1Cu^4_1Cu^6_1Cu^7_1Cu^5_1Cu^2_3Zr^8_2Zr^3_3$	12	110.099	1.631	0.906	0.171	$Cu_4Zr_{3/2}$	$[Cu_8Zr_5](Cu_{16/3})$
	Cu^2	9.76	$Cu_{10}Zr_4$	$Cu^2Cu^5_2Cu^4_1Cu^1_3Zr^3_2Zr^8_2Cu^6_1Cu^2_1Cu^7_1$	13	123.516	1.830	0.929	0.147	$Cu_4Zr_{3/2}$	$[Cu_{10}Zr_4](Cu_{2/3})$
	Zr^3	12.72	Zr_3Cu_{12}	$Zr^3Cu^2_2Cu^7_2Cu^5_1Cu^6_2Cu^4_2Cu^1_3Zr^3_2$	14	107.354	1.591	1.207	0.163	$Zr_{3/2}Cu_4$	$[Zr_3Cu_{12}](Zr_{3/2})$
	Cu^4	13.26	Cu_8Zr_5	$Cu^4Cu^7_1Cu^6_1Cu^5_1Cu^1_2Cu^2_2Zr^3_4Zr^8_1$	12	121.717	1.804	0.906	0.165	Cu_8Zr_3	$[Cu_8Zr_5](Cu_{16/3})$
	Cu^5	12.70	$Cu_{11}Zr_3$	$Cu^5Cu^6_2Cu^4_2Cu^1_2Cu^2_4Cu^6_1Zr^3_2Zr^8_1$	13	125.955	1.866	0.945	0.165	Cu_8Zr_3	$[Cu_{11}Zr_3](Zr_{9/8})$
	Cu^6	11.92	Cu_8Zr_5	$Cu^6Cu^3_2Cu^4_1Cu^1_2Cu^2_2Zr^3_4Zr^8_1$	12	107.158	1.588	0.906	0.209	Cu_8Zr_3	$[Cu_8Zr_5](Cu_{16/3})$
	Cu^7	10.91	Cu_6Zr_6	$Cu^7Cu^4_1Cu^2_2Zr^8_2Zr^3_4Cu^2_2$	11	92.062	1.364	0.88	0.219	Cu_8Zr_3	$[Cu_6Zr_6](Cu_{10})$
	Zr^8	11.72	Zr_5Cu_{13}	$Zr^8Cu^7_2Cu^1_4Cu^2_4Cu^5_1Cu^4_1Cu^6_1Zr^3_4$	17	88.270	1.308	1.181	0.272	Zr_3Cu_8	$[Zr_5Cu_{13}](Cu_{1/3})$
$CuZr_2$	Cu^1	4.82	Cu_5Zr_8	$Cu^1Zr^1_8Cu^1_4$	12	91.633	1.792	0.857	0.102	Cu_1Zr_2	$[Cu_5Zr_8](Zr_2)$
	Zr^1	14.04	Zr_9Cu_4	$Zr^1Cu^1_4Zr^1_8$	12	91.633	1.792	1.071	0.102	$Zr_1Cu_{1/2}$	$[Zr_9Cu_4](Cu_{1/2})$
Cu_5Zr_8	Cu^1	5.11	Cu_3Zr_{10}	$Cu^1Zr^5_4Zr^6_4Cu^1_2Zr^4_2$	12	80.828	1.527	0.828	0.182	Cu_5Zr_8	$[Cu_3Zr_{10}](Cu_{13/4})$
	Cu^2	9.18	Cu_4Zr_8	$Cu^2Zr^5_2Zr^7_4Cu^3_1Zr^4_2Cu^2_2$	11	86.672	1.637	0.846	0.158	$Cu_{5/2}Zr_4$	$[Cu_4Zr_8](Cu)$
	Cu^3	6.55	Cu_4Zr_9	$Cu^3Cu^2_1Zr^6_4Zr^5_2Zr^7_2Cu^3_2Zr^4_1$	12	89.032	1.682	0.842	0.150	$Cu_{5/2}Zr_4$	$[Cu_4Zr_9](Cu_{13/8})$
	Zr^4	9.65	$Zr_{11}Cu_4$	$Zr^4Cu^2_2Zr^5_2Zr^6_2Zr^7_4Zr^4_2Cu^3_1Cu^1_1$	14	92.439	1.746	1.061	0.149	$Zr_4Cu_{5/2}$	$[Zr_{11}Cu_4](Cu_{23/8})$
	Zr^5	13.02	Zr_6Cu_6	$Zr^5Cu^2_2Cu^1_2Cu^3_2Zr^4_2Zr^6_2Zr^5_2$	11	86.672	1.637	1.122	0.158	$Zr_4Cu_{5/2}$	$[Zr_6Cu_6](Zr_{18/5})$
	Zr^6	10.25	Zr_9Cu_6	$Zr^6Cu^3_4Cu^1_2Zr^4_2Zr^5_2Zr^6_3Zr^7_1$	14	68.175	1.288	1.094	0.252	$Zr_4Cu_{5/2}$	$[Zr_9Cu_6](Cu_{3/5})$
	Zr^7	10.20	Zr_7Cu_6	$Zr^7Cu^2_4Cu^3_2Zr^4_4Zr^7_2$	12	80.113	1.513	1.111	0.183	$Zr_4Cu_{5/2}$	$[Zr_7Cu_6](Zr_{13/5})$
$Cu_{10}Zr_7$	Cu^1	9.40	Cu_5Zr_6	$Cu^1Cu^2_1Zr^4_2Zr^2_1Zr^3_1Cu^4_2Cu^5_1Zr^1_1Zr^5_1$	10	79.762	1.318	0.870	0.310	$Cu_5Zr_{7/2}$	$[Cu_5Zr_6](Cu_5Zr)$
	Cu^2	9.42	Cu_5Zr_6	$Cu^2Cu^1_1Zr^1_1Cu^5_1Zr^4_2Cu^3_2Zr^5_1Zr^2_1Zr^3_1$	10	113.990	1.883	0.870	0.223	$Cu_5Zr_{7/2}$	$[Cu_5Zr_6](Cu_5Zr)$
	Cu^3	9.37	Cu_5Zr_6	$Cu^3Zr^4_2Zr^1_1Cu^5_1Cu^2_2Zr^5_1Zr^2_1Zr^3_1Cu^4_1$	10	117.397	1.939	0.870	0.055	$Cu_5Zr_{7/2}$	$[Cu_5Zr_6](Cu_5Zr)$
	Cu^4	9.34	Cu_5Zr_6	$Cu^4Zr^1_2Zr^4_2Cu^5_1Cu^1_2Cu^3_1Zr^5_1Zr^2_1Zr^3_1$	10	109.851	1.815	0.870	0.078	$Cu_5Zr_{7/2}$	$[Cu_5Zr_6](Cu_5Zr)$
	Cu^5	8.33	Cu_6Zr_5	$Cu^5Cu^4_1Zr^3_3Cu^2_1Cu^3_1Zr^3_1Zr^2_1Cu^5_1Cu^1_1$	10	83.052	1.372	0.889	0.151	$Cu_5Zr_{7/2}$	$[Cu_6Zr_5](Cu_4Zr_2)$
	Zr^4	14.63	Zr_7Cu_{10}	$Zr^4Cu^1_2Cu^3_2Cu^4_2Cu^2_2Zr^5_2Zr^3_2Zr^2_2Cu^5_2$	16	78.131	1.291	1.143	0.347	$Zr_{7/2}Cu_5$	$[Zr_7Cu_{10}]$
	Zr^5	11.10	Zr_7Cu_{10}	$Zr^5Cu^3_3Cu^3_2Cu^2_2Cu^4_2Cu^1_1Zr^4_2Zr^1_2Zr^2_1Zr^3_1$	16	76.838	1.269	1.143	0.233	$Zr_{7/2}Cu_5$	$[Zr_7Cu_{10}]$
	Zr^1	16.84	Zr_5Cu_8	$Zr^1Cu^4_2Cu^2_2Cu^3_2Cu^1_2Zr^5_4$	12	76.57	1.265	1.154	0.227	Zr_7Cu_{10}	$[Zr_5Cu_8](Cu_2Zr_2)$
	Zr^2	12.68	$ZrCu_{10}$	$Zr^2Cu^1_2Cu^3_2Cu^2_2Cu^4_2Cu^5_2$	10	113.534	1.875	1.25	0.137	Zr_7Cu_{10}	$[ZrCu_{10}](Zr_6)$
	Zr^3	12.69	$ZrCu_{10}$	$Zr^3Cu^1_2Cu^3_2Cu^2_2Cu^2_2Cu^4_2$	10	110.794	1.830	1.25	0.051	Zr_7Cu_{10}	$[ZrCu_{10}](Zr_6)$

of the Cu_8Zr_3 phase have been calculated and are listed in Table 1. As can be seen, the Cu^4 atom has the largest IFCs of 13.26 eV Å^{-2}, suggesting that it possesses the strongest interaction with near-neighbor atoms, and further it can be considered as the central atom of the cluster on the basis of our new rule. The Cu^2 atom has the smallest IFCs of 9.76 eV Å^{-2}, reflecting that the interactions between these atoms are weaker, and they serve as the glue atoms of the model. As for the other atoms (namely Cu^1, Zr^3, Cu^5, Cu^6, Cu^7 and Zr^8), because their corresponding IFCs lie between the maximum and minimum IFCs values, they may act either as the shell atoms of the cluster or as the glue atoms in the "cluster-plus-glue-atom" model. Therefore, the characteristic principal cluster of the Cu_8Zr_3 phase is determined as the Cu^4-centered CN12 Cu_8Zr_5 cluster. Interestingly, many theoretical and experimental studies [19,21,40,42,63,76,77] have reported that there indeed exists certain short-range ordered structures derived from the Cu_8Zr_5 icosahedral cluster in CuZr-based amorphous alloys (as shown in Fig. 4). These results indicated that the proposed new rule is reasonable for determining the characteristic principal cluster in the "cluster-plus-glue-atom" model. Besides, the calculated total energy of the Cu^4-centered CN12 Cu_8Zr_5 cluster is the lowest among the eight

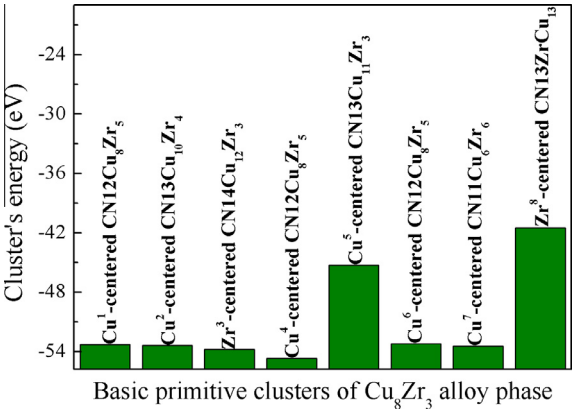

Fig. 2. The energy of the basic primitive clusters in the Cu_8Zr_3 alloy phase.

basic primitive clusters in the Cu_8Zr_3 phase (as shown in Fig. 2 and Supplementary Table S2) [78], which suggested that the Cu^4-centered CN12 Cu_8Zr_5 icosahedral cluster is the most energetically favorable cluster, with an efficiently close-packed geometry. This result also verifies the reliability of our new rule for determining the characteristic principal clusters. Moreover, the atomic radius ratio R_0/R_1 of the central atom vs. the first-shell atoms for this Cu_8Zr_5 cluster is calculated to be 0.906. This is a deviation of only 0.4% from the ideal value of 0.902 (i.e. the ideal close-packed icosahedral cluster) [2], which further demonstrates that the Cu_8Zr_5 icosahedral cluster is quite close to the ideal close-packing.

The characteristic principal clusters for the other seven intermetallic compounds in the Cu–Zr alloy system (i.e. Cu_5Zr, $CuZr_2$, CuZr, Cu_2Zr, Cu_5Zr_8 $Cu_{51}Zr_{14}$, $Cu_{10}Zr_7$) and the nine intermetallic compounds in the Al–Ni–Zr alloy system (i.e. Al_2NiZr_6, AlNiZr, Al_5Ni_2Zr, $AlNi_2Zr$, Al_3Ni_5, Al_3Zr_5, $AlNi_3$, $AlZr_3$, AlNi) have been studied using similar methods [75,79]. The optimized lattice parameters and available experimental values for these alloy phases are listed in Table S1. The characteristic principal

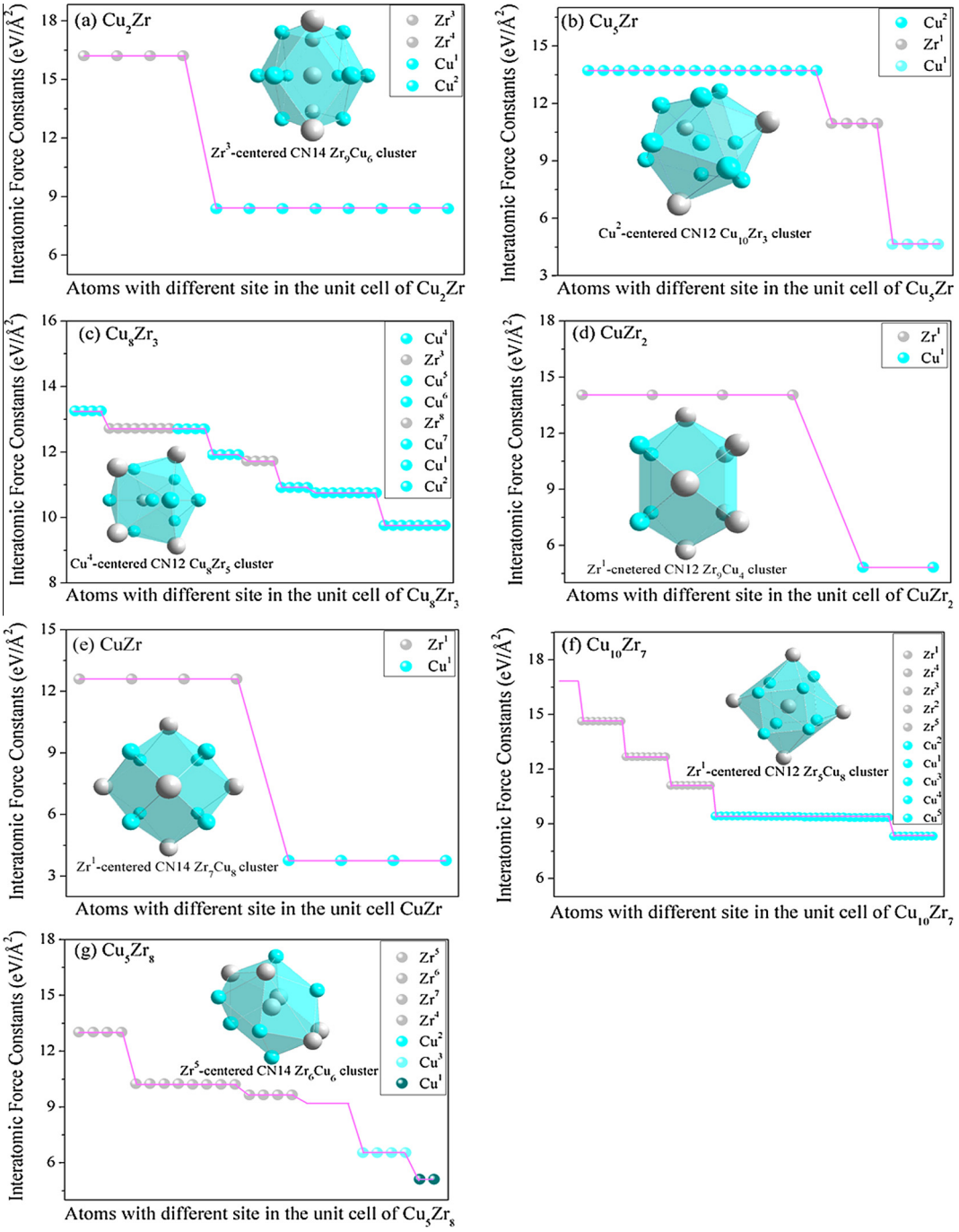

Fig. 3. The characteristic principal clusters of alloy phases in Cu–Zr binary systems, determined by the new rule.

clusters obtained for Cu–Zr intermetallic compounds are presented Table 1, and are also depicted in Fig. 3. It can be seen that the characteristic principal cluster for the Cu_2Zr, Cu_5Zr, $CuZr_2$, CuZr, $Cu_{10}Zr_7$, Cu_5Zr_8 and $Cu_{51}Zr_{14}$ phases are CN14 Zr_5Cu_{10}, CN12 $Cu_{10}Zr_3$, CN12 Zr_9Cu_4, CN14 Zr_7Cu_8, CN12 Zr_5Cu_8, CN11 Zr_6Cu_6 and CN12 Cu_9Zr_4, respectively; their corresponding cluster formulas are $[Zr_5Cu_{10}]$, $[Cu_{10}Zr_3](Cu_5)$, $[Zr_9Cu_4](Cu_{1/2})$, $[Zr_7Cu_8](Zr)$, $[Zr_5Cu_8](Cu_2Zr_2)$, $[Zr_6Cu_6](Zr_{18/5})$ and $[Cu_9Zr_4](Cu_{39/7})$. Likewise, the corresponding characteristic principal clusters of the nine intermetallic compounds in Al–Ni–Zr alloy system have also been determined (see Table S3 and Fig. S4). The results indicate that the characteristic principal clusters for the Al_2NiZr_6, AlNiZr, Al_5Ni_2Zr, $AlNi_2Zr$, Al_3Ni_5, Al_3Zr_5, $AlNi_3$, $AlZr_3$ and AlNi phases are CN11 Ni_3Zr_9, CN11 $Ni_3Al_3Zr_6$, CN14 $ZrAl_{12}Ni_2$, CN14 $ZrNi_8Al_6$, CN12 Al_5Ni_8, CN10 Al_3Zr_8, CN12 Ni_9Al_4, CN12 Zr_9Al_4 and CN14 Al_7Ni_8, respectively; hence their corresponding cluster formulas are $[Ni_3Zr_9](Al_6Zr_9)$, $[Ni_3Al_3Zr_6](Ni_3Al_3)$, $[ZrAl_{12}Ni_2](Ni_{14/5}Zr_{7/5})$, $[ZrNi_8Al_6](Ni_4Zr_5)$, $[Al_5Ni_8](Ni_{1/3})$, $[Al_3Zr_8](Al_{9/5})$, $[Ni_9Al_4](Ni_3)$, $[Zr_9Al_4](Zr_3)$ and $[Al_7Ni_8](Al)$. Most of the predicted characteristic principal clusters (i.e. Zr_5Cu_{10}, Zr_7Cu_8, Cu_8Zr_5, Cu_6Zr_6, Zr_9Cu_4 and Cu_9Zr_4 clusters) in the Cu–Zr binary system accord with Tian et al.'s theoretical works [34,76]. Our predicted characteristic principal clusters for the Al–Ni–Zr alloy system are also in good agreement with the available theoretical results of Dong and colleagues [19,20,33,52–54]; detailed results and discussion are provided in the Supplementary materials. The conformity between our research and the available existing results proves the feasibility of using the new rule to determine characteristic principal clusters in the "cluster-plus-glue-atom" model.

5. Conclusion and outlook

We have developed a new method to determine the characteristic principal clusters for the "cluster-plus-glue-atom" model. Since the interaction between atoms inside the cluster is stronger than that between the clusters corresponding to the glue atoms, the parameter IFCs, which can be applied to reflect the interactions between atoms, is proposed to describe the cluster-based model. Through the calculation and analysis of the IFCs of an alloy phase, the central atom as well as the shell atoms of the cluster and the glue atoms can be clearly distinguished. The characteristic principal cluster that best represents the structural feature of the phase can then finally be determined by combining the existing rules. The alloy phases in Cu–Zr and Al–Ni–Zr systems were checked to validate this new rule in applications. The results indicated that the characteristic principal cluster of an alloy phase can be effectively established via this approach. Our investigations will help people to better understand the rules of selecting the right characteristic principal clusters for the "cluster-plus-glue-atom" model, and hence will make it more convenient to apply this cluster-based model.

Although the "cluster-plus-glue-atom" model can easily describe the structure of complex metallic alloy phases, the biggest obstacle limiting its application is that it is difficult to determine the characteristic principal cluster. The new rule proposed in this work can be used to effectively determine the characteristic principal cluster; sequentially, it paves the way for the applications of the "cluster-plus-glue-atom" model. By combining our new rule with the "cluster-plus-glue-atom" model, the following three issues are expected to be resolved.

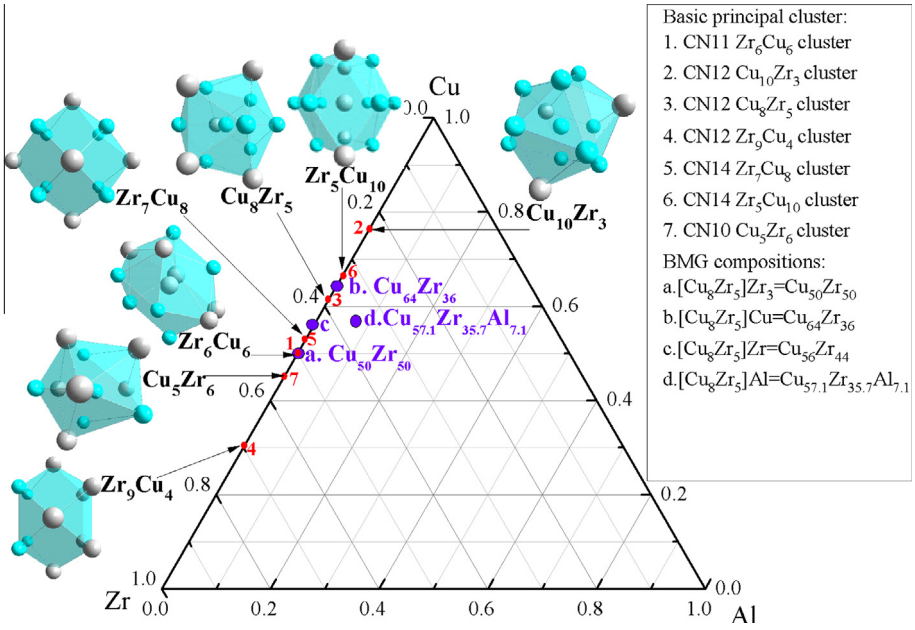

Fig. 4. The characteristic principal clusters in the binary Cu–Zr alloy system, along with the correlations between CN12 Cu_8Zr_5 icosahedral cluster and CuZr-based bulk metallic glasses reflected in the Cu–Zr–Al ternary phase diagram.

(1) Composition design of bulk metallic glasses (BMGs): considering the correlations between the glass forming ability of BMGs and their internal atomic structures reflected by the principal clusters [80–84], the composition of BMGs can be designed on the basis of the characteristic principal clusters. For example, since the good glass-forming alloys in the Cu–Zr system are closely related to the icosahedral clusters, via the Cu_8Zr_5 icosahedral cluster plus a third element as glue atoms, a series of Cu_8Zr_5-based ternary BMGs has been successfully designed and synthesized [27,40]; the optimal glass forming compositions $Cu_{50}Zr_{50}$, $Cu_{64}Zr_{36}$ and $Cu_{56}Zr_{44}$ can also be designed by the Cu_8Zr_5 cluster plus the glue atom Cu or Zr [34,76], as reflected in Fig. 4.

(2) Description of the short-range ordered structure in complex metallic alloys: because the short-range orders in the structure of complex metallic alloys are viewed as the efficient packing of relevant characteristic principal clusters [85–88], the short-range ordered structure in complex metallic alloys can be described by their corresponding characteristic principal clusters. As shown in Fig. 4, the experimentally synthesized amorphous alloy $Cu_{57.1}Zr_{35.7}Al_{7.1}$ can be described as the Cu_8Zr_5 characteristic principal cluster plus the glue atom Al [21,63], implying that certain short-range orders deriving from the Cu_8Zr_5 icosahedral cluster exist in $Cu_{57.1}Zr_{35.7}Al_{7.1}$ structure.

(3) Relationship between the cluster structures of complex metallic alloys and their mechanical properties: the characteristic principal clusters are regarded as the basic building units of complex metallic alloys; meanwhile, the different characteristic principal clusters have different IFCs, and the IFCs are directly related to mechanical properties [89–94]. Therefore, it is anticipated to find the relationship between the cluster structures of complex metallic alloys and their mechanical properties, and this also is our further research direction.

Acknowledgements

This work was supported by the National Natural Science Foundation of China (Grant Nos. 51121061, 51131002, 51372215), the Key Basic Research Program of Hebei Province of China (Grant No. 12965135D) and the Natural Science Foundation for Distinguished Young Scholars of Hebei Province of China (Grant No. E2013203265). R.M. acknowledges the support from the NSERC and CRC programs, Canada. The authors also would like to thank the staff of the Center for Computational Materials Science, Institute for Materials Research, Tohoku University for computer support. Y.K. is thankful to the CREST project headed by Prof. M. Kotani.

Appendix A. Supplementary data

Supplementary data associated with this article can be found, in the online version, at http://dx.doi.org/10.1016/j.actamat.2014.04.052.

References

[1] Mackay AL, Finney JL. J Appl Crystallogr 1973;6:284.
[2] Miracle DB, Sanders WS, Senkov ON. Philos Mag 2003;83:2409.
[3] Miracle DB. Nat Mater 2004;3:697.
[4] Miracle DB. J Non-Cryst Solids 2004;342:89.
[5] Miracle DB. Acta Mater 2006;54:4317.
[6] Wang AP, Wang JQ, Ma E. Appl Phys Lett 2007;90:121912.
[7] Boudreaux DS. Phys Rev B 1978;18:4039.
[8] Levine D, Steinhardt PJ. Phys Rev Lett 1984;53:2477.
[9] Nurgayanov PP, Chudinov VG. Glass Phys Chem 2000;26:335.
[10] Waniuk T, Schroers J, Johnson WL. Phys Rev B 2003;67:184203.
[11] Hirata A, Guan PF, Fujita T, Hirotsu Y, Inoue A, Yavari AR, et al. Nat Mater 2011;10:28.
[12] Dubois JM. In: Belin-Ferre E, editor. Book series in complex metallic alloys, vol. 1. Singapore: World Scientific; 2008. p. 88.
[13] Yuan L, Pang C, Wang YM, Qiang JB, Dong C. Intermetallics 2010;18:1800.
[14] Mechler S, Schumacher G, Koteski V, Riesemeier H, Schaders F, Mahnke HE. Appl Phys Lett 2010;97:041914.
[15] Hao CP, Wang Q, Ma RT, Wang YM, Qiang JB, Dong C. Acta Phys Sin 2011;60:116101.
[16] Dong C, Wang YM, Qiang JB, Wang Q. Chin J Nat 2011;33:322.
[17] Zhang C, Tian H, Hao CP, Zhao JJ, Wang Q, Liu EX, et al. J Mater Sci 2013;48:3138.
[18] Dong C, Qiang JB, Wang YM, Jiang N, Wu J, Thiel P. Philos Mag 2006;86:263.
[19] Dong C, Wang Q, Qiang JB, Wang YM, Jiang N, Han G, et al. J Phys D: Appl Phys 2007;40:273.
[20] Dong C, Qiang JB, Yuan L, Wang Q, Wang YM. Chin J Nonferrous Met 2011;21:2502.
[21] Han G, Qiang JB, Li FW, Yuan L, Quan SG, Wang Q, et al. Acta Mater 2011;59:5917.
[22] Smith WF. Foundations of materials science and engineering. New York: McGraw-Hill; 1992.
[23] Wiliam D, Callister J. Materials science and engineering: an introduction. 5th ed. New York: Wiley; 1999.
[24] Askeland DR, Phule PP. The science and engineering of materials. 4th ed. USA, Stamford, CT: Thomson Learning; 2004.
[25] Hu GX, Cai X, Rong YH. Fundam Mater Sci 2006:19.
[26] Sheng HW, Luo WK, Alamgir FM, Bai JM, Ma E. Nature 2006;439:419.
[27] Xia JH, Qiang JB, Wang YM, Wang Q, Dong C. Appl Phys Lett 2006;88:101907.
[28] Keys AS, Glotzer SC. Phys Rev Lett 2007;99:235503.
[29] Saida JJ, Sanada TK, Sato S, Imafuku M, Inoue A. Appl Phys Lett 2007;91:111901.
[30] Ma RT, Hao CP, Wang Q, Ren MF, Wang YM, Dong C. Acta Metall Sin 2010;46:1034.
[31] Wang YM, Wang Q, Zhao JJ. Scr Mater 2010;63:178.
[32] Chen H, Qiang JB, Wang Q, Wang YM, Dong C. Isr J Chem 2011;51:1226.
[33] Chen JX, Wang Q, Dong C. Rare Metal Mater Eng 2011;40:69.
[34] Tian H, Zhang C, Wang L, Zhao JJ, Dong C, Wen B, et al. J Appl Phys 2011;109:123520.
[35] Wang Q, Ji CJ, Wang YM, Qiang JB, Dong C. Metall Mater Trans 2013;44A:1872.
[36] Henley CL. J Non-Cryst Solids 1985;75:91.
[37] Ma Y, Stern EA, Gayle FW. Phys Rev Lett 1987;58:1956.

[38] Tendeloo G, Landuyt J, Amelinckx S, Ranganathan S. J Microsc 1988;149:1.
[39] Ma Y, Stern EA. Phys Rev B 1988;38:3754.
[40] Yang L, Xia JH, Wang Q, Dong C, Chen LY, Ou X, et al. Appl Phys Lett 2006;88:241913.
[41] Lee SC, Lee CM, Lee JC, Kim HJ, Shibutani Y, Fleury E. Appl Phys Lett 2008;92:151906.
[42] Sha ZD, Xu B, Shen L, Zhang AH, Feng YP, Li Y. J Appl Phys 2010;107:063508.
[43] Jakse N, Pasturel A. Phys Rev B 2008;78:214204.
[44] Shen YT, Kim TH, Gangopadhyay AK, Kelton KF. Phys Rev Lett 2009;102:057801.
[45] Mendelev MI, Kramer MJ, Ott RT, Sordelet DJ, Besser MF, Kreyssig A. Philos Mag 2010;90:3795.
[46] Almyras GA, Papageorgiou DG, Lekka ChE, Mattern N, Eckert J, Evangelakis GA. Intermetallics 2011;19:657.
[47] Turnbull D. Contemp Phys 1969;10:473.
[48] Kreuch G, Hafner J. J Non-Cryst Solids 1995;189:227.
[49] Wang O, Zhu CL, Li YH, Cheng X, Chen WR, Wu J. J Mater Res 2008;23:1543.
[50] Dong C, Wang YM, Qiang JB. Mater Trans JIM 2004;45:1177.
[51] Dong C, Wang Q, Qiang JB. Appl Phys 2007;40:273.
[52] Chen JX, Wang Q, Wang YM, Qiang JB, Dong C. Philos Mag Lett 2010;90:683.
[53] Chen JX, Dong C, Wang Q. Chem Phys Lett 2011;502:176.
[54] Chen JX, Qiang JB, Wang Q, Dong C. Acta Phys Sin 2012;61:046102.
[55] Luo LJ, Wu J, Wang Q, Wang YM, Han G, Dong C. Philos Mag 2010;90:3961.
[56] Steinhardt PJ. Nature 2008;452:43.
[57] Altounian Z, Guo-hua Tu, Strom-Olsen JO. J Appl Phys 1982;53:4755.
[58] Park KW, Lee CM, Wakeda M, Shibutani Y, Falk ML, Lee JC. Acta Mater 2008;56:5440.
[59] Kaban I, Jovari P, Kokotin V, Shuleshova O, Beuneu B, Saksl K, et al. Acta Mater 2013;61:2509.
[60] Inoue A, Zhang T, Masumoto T. Mater Trans JIM 1990;31:177.
[61] Li YH, Zhang W, Dong C, Qiang JB, Makino A, Inoue A. Intermetallics 2010;18:1.
[62] Miracle DB, Lord EA, Ranganathan S. Mater Trans JIM 2006;47:1737.
[63] Wang Q, Dong C, Qiang JB, Wang YM. Mater Sci Eng A 2007;18:449.
[64] Lopez JM, Alonso JA, Gallego LJ. Phys Rev B 1987;36:3716.
[65] Greer AL. Science 1995;267:1947.
[66] Inoue A. Mater Sci Forum 1998;855:269.
[67] de Boer FR, Boom R, Mattens WCM, Miedema AR, Niessen AK. In: de Boer FR, Pettifor DG, editors. Cohesion in metals: transition metal alloys, vol. 1. Amsterdam: North-Holland; 1988.
[68] Diaz-Sanchez LE, Romero AH, Gonze X. Phys Rev B 2007;76:104302.
[69] Gonze X, Charlier JC, Allan DC, Teter MP. Phys Rev B 1994;50:13035.
[70] Quong AA. Phys Rev B 1994;49:3226.
[71] Kumar V. J Phys Chem Solids 2009;61:91.
[72] Gonze X, Lee C. Phys Rev B 1997;55:10355.
[73] See, for example Brovman EG, Kagan YM. In: Horton GK, Maradudin AA, editors. Dynamical properties of solids, vol. 1. Amsterdam: North-Holland; 1974. p. 247.
[74] Kresse G, Marsman M, Furthüller J. VASP: the guide. <http://cms.mpi.Univie.ac.at/vasp/>.
[75] Villars P, Calvert LD. Pearson's handbook of crystallographic data for intermetallic phases. Materials Park, OH: ASM International; 1997.
[76] Tian H, Liao YL, Zhang C, Zhao JJ, Wen B, Wang Q, et al. Sci China Phys Mech Astron 2011;54:249.
[77] Hume-Rothery W, Anderson E. Philos Mag 1960;5:383.
[78] Hirata A, Kang LJ, Fujita T, Klumov B, Matsue K, Kotani M, et al. Science 2013;341:376.
[79] Du JL, Wen B, Melnik R, Kawazoe Y. J Alloys Compd 2014;588:96.
[80] Yang L, Guo GQ, Chen YL, Huang CL, Ge T, Chen D, et al. Phys Rev Lett 2012;109:105502.
[81] Li Y, Guo Q, Kalb JA, Thompson CV. Science 2008;322:1816.
[82] Yu CY, Liu XJ, Lu J, Zheng GP, Liu CT. Sci Rep 2013;3:2124.
[83] Yu P, Bai HY, Wang WH. J Mater Res 2006;21:1674.
[84] An Q, Samwer III K, Goddard WA, Johnson WL, Jaramillo-Botero A, Garret G, et al. J Phys Chem Lett 2012;3:3143.
[85] Liu ACY, Neish MJ, Stokol G, Buckley GA, Smillie LA, de Jonge MD, et al. Phys Rev Lett 2013;110:205503.
[86] Cheng YQ, Ma E. Prog Mater Sci 2011;56:379.
[87] Ward L, Miracle D, Windl W, Senkov ON, Flores K. Phys Rev B 2013;88:134205.
[88] Antonowicz J, Pietnoczka A, Drobiazg T, Almyras GA, Papageorgiou DG, Evangelakis GA. Phil Mag 2012;92:1856.
[89] Ding J, Cheng YQ, Ma E. Acta Mater 2014;69:343.
[90] Cheng YQ, Sheng HW, Ma E. Phys Rev B 2008;78:014207.
[91] Mendelev MI, Rehbein DK, Ott RT, Kramer MJ, Sordelet DJ. J Appl Phys 2007;102:093518.
[92] Duan G, Xu DH, Zhang Q, Zhang GY, Cagin T, Johnson WL, et al. Phys Rev B 2005;71:224208.
[93] Wu ZW, Li MZ, Wang WH, Liu KX. Phys Rev B 2013;88:054202.
[94] Cheng YQ, Ma E, Sheng HW. Phys Rev Lett 2009;102:245501.